

Large quantum nonreciprocity in plasmons dragged by drifting electrons

Debasis Dutta^{1,*} and Amit Agarwal^{1,†}

¹*Department of Physics, Indian Institute of Technology Kanpur, Kanpur-208016, India*

(Dated: July 9, 2024)

Collective plasmon modes, riding on top of drifting electrons, acquire a fascinating nonreciprocal dispersion characterized by $\omega_p(\mathbf{q}) \neq \omega_p(-\mathbf{q})$. The classical plasmonic Doppler shift arises from the polarization of the Fermi surface due to the applied DC bias voltage. Here, we predict an additional quantum contribution to the plasmonic Doppler shift originating from the quantum metric of the Bloch wavefunction. We systematically compare the classical and quantum corrections to the Doppler shifts by investigating the drift-induced nonreciprocal plasmon dispersion in graphene and in twisted bilayer graphene. We show that the quantum plasmonic Doppler shift dominates in moiré systems at large wavevectors, yielding plasmonic nonreciprocity up to 20% in twisted bilayer graphene. Our findings highlight the significance of the quantum corrections to plasmonic Doppler shift in moiré systems and motivate the design of innovative nonreciprocal photonic devices with potential technological implications.

I. Introduction

Light propagates symmetrically in opposite directions in conventional optical systems. This is a consequence of the time-reversal invariance of Maxwell's equations or Lorentz's reciprocity principle [1–4]. Breaking reciprocity for asymmetric light propagation is conventionally done by magneto-optical approaches, which require large magnetic fields and limit the efficiency for nanoscale devices and on-chip integration [5]. To remedy this, nonreciprocal plasmonics in atomically thin two-dimensional (2D) materials, such as graphene, present opportunities for direction-dependent light propagation at the nanoscale. This is crucial for enabling compact devices in classical and quantum information processing, nonreciprocal devices for Faraday rotation, isolation, one-way waveguiding, and nonreciprocal cavities [6–8]. These make them a valuable addition to the nanophotonics toolbox [9–11].

Nonreciprocity in bulk plasmon dispersion can intrinsically arise in noncentrosymmetric magnetic materials. This is induced either by the dipolar distribution of the quantum metric or by the ‘chiral Berry’ plasmons at the boundary of magnetic materials [12–15]. A more promising and controllable route for extrinsic breaking of Lorentz reciprocity is biasing the plasmonic material with a direct current. This induces nonreciprocal plasmons with a dispersion that differs for plasmon propagating along or opposite to the direction of the drifting carriers. This approach is minimally invasive for on-chip architectures, and it is known as the plasmonic Fizeau drag or Doppler effect [8, 16–20]. Drift-induced nonreciprocal plasmons in single-layer graphene (SLG) have been recently predicted and demonstrated [16, 18, 21–24]. Using near-field imaging techniques, the plasmonic Doppler shift was measured for SLG [16, 17] with a wavelength shift, $\delta\lambda_p/\lambda_p \approx 2\%$ for electron drift velocity,

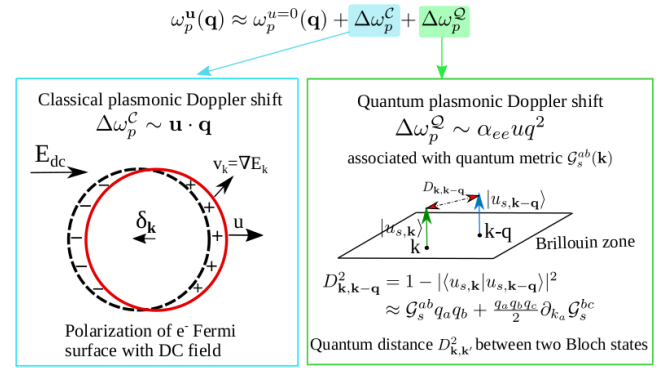


FIG. 1. The drift-induced nonreciprocal plasmon dispersion has both classical and quantum contributions. The classical frequency shift $\Delta\omega_p^C$ arises from the polarization of the Fermi surface induced by the DC electric field. The solid and dashed line represents the Fermi surface in the absence and presence of drift flow (u) of carriers. The quantum plasmonic Doppler shift, $\Delta\omega_p^Q$, arises from the quantum metric $G_s^{ab}(\mathbf{k})$ of the electron wavefunction in the presence of drifting charge carriers. The quantum metric is linked with the notion of quantum distance, $D_{\mathbf{k},\mathbf{k}-\mathbf{q}}^2$ between two Bloch states at different momentum, \mathbf{k} and $\mathbf{k}-\mathbf{q}$, respectively.

$u/v_F \approx 17\%$ (given $v_F = 0.86 \times 10^6$ m/s) [16]. These studies are primarily focussed on the classical plasmonic Doppler shift, which primarily arises from the displacement of the Fermi surface due to drift flow (see Fig. 1) [16, 18, 21–24]. Additionally, the possibility of a quantum Doppler shift has been recently proposed in moiré system owing to the band hybridization [19].

Motivated by these studies, we predict an exciting quantum Doppler shift-induced plasmonic nonreciprocity, which originates from the quantum metric - a band geometric property of the electron wavefunctions (see Fig. 1). Our investigation reveals that the classical correction varies linearly with the wavevector, while the quantum correction varies quadratically with the wavevector, as depicted in Fig. 1. We show that as

* ddebasis@iitk.ac.in

† amitag@iitk.ac.in

flat band moiré systems have a large effective interaction strength and undamped plasmons at large wavevectors, twisted bilayer graphene (TBG) can support a large plasmonic nonreciprocity ($\sim 20\%$) driven by quantum correction. As a consequence, moiré materials in general and TBG in particular offers highly tunable platforms for observing and designing devices based on nonreciprocal light propagation [25–29].

II. Nonreciprocal plasmons with DC bias

The optical and plasmonic properties of a quantum system can be described by the dynamical density-density response function in the linear response of the applied electric field [30–32]. Plasmons are calculated from the zeros of the real part of the dielectric function. Within random-phase approximation (RPA), the dynamical dielectric function is calculated as [30, 33, 34]

$$\epsilon(\mathbf{q}, \omega) = 1 - V_q \Pi(\mathbf{q}, \omega). \quad (1)$$

Here, $V_q = 2\pi e^2 / (\kappa |\mathbf{q}|)$ denotes the 2D Fourier transform of the Coulomb potential, κ denotes an effective background dielectric constant, and $\Pi(\mathbf{q}, \omega)$ represents dynamical density-density response function [30, 32, 35].

We will treat the effect of externally applied DC current in a non-perturbative fashion by capturing its impact on the Fermi-Dirac distribution function [19, 21, 22]. In the hydrodynamic limit, we can model the drifting carrier distribution function as [16, 36, 37]

$$\tilde{f}_{s,\mathbf{k}} = \left\{ \exp \left[\frac{E_{s,\mathbf{k}} - \mathbf{u} \cdot \mathbf{k} - \mu}{k_B T} \right] + 1 \right\}^{-1}, \quad (2)$$

which nullifies the energy and momentum conserving electron-electron collision integral [36]. Here, \mathbf{u} denotes the drift velocity of the quasiparticles, T denotes temperature, μ denotes the chemical potential, and $E_{s,\mathbf{k}}$ denotes Bloch band energy at crystal momentum \mathbf{k} with band index s of the system. This drifting carrier distribution function induces a shift of the Fermi surface by momentum $\delta_{\mathbf{k}} = -m_{\text{eff}} \mathbf{u}$, in the small $u = |\mathbf{u}|$ limit [19] (see Sec. S1 of the Supplemental Material (SM) [38] for details). Here, m_{eff} denotes the effective mass of the quasiparticles.

Using this approach, we can express the DC current-driven non-interacting density-density response function for a 2D system as [21, 30, 39]

$$\Pi(\mathbf{q}, \omega) = g_s \sum_{s,s'} \int \frac{d^2 \mathbf{k}}{(2\pi)^2} \frac{(\tilde{f}_{s,\mathbf{k}+\mathbf{q}} - \tilde{f}_{s',\mathbf{k}}) F_{\mathbf{k}+\mathbf{q},\mathbf{k}}^{ss'}}{E_{s,\mathbf{k}+\mathbf{q}} - E_{s',\mathbf{k}} - \omega - i\eta}. \quad (3)$$

Here, $\tilde{f}_{s,\mathbf{k}}$ is the modified Fermi-Dirac distribution function at momentum \mathbf{k} with band energies $E_{s,\mathbf{k}}$, g_s denotes the total degeneracy factor, and η is the broadening parameter. Here, the important quantity is the band coherence factor $F_{\mathbf{k}+\mathbf{q},\mathbf{k}}^{ss'} = |\langle u_{s,\mathbf{k}+\mathbf{q}} | u_{s',\mathbf{k}} \rangle|^2$, which

describes the overlap between two energy eigenstates at momentum \mathbf{k} and $\mathbf{k} + \mathbf{q}$. We set $\hbar = 1$ throughout our calculations and explicitly mention it when needed.

We first investigate the long-wavelength limit ($q \ll k_F$, where k_F denotes the Fermi wavevector) of the intraband plasmon dispersion in the presence of drift flow. For that, we expand the intraband band-overlap factor, $F_{\mathbf{k},\mathbf{k}+\mathbf{q}}^{ss}$ up to $\mathcal{O}(q^3)$ [13, 40], and obtain

$$F_{\mathbf{k}+\mathbf{q},\mathbf{k}}^{ss} \approx 1 - q_a q_b \mathcal{G}_s^{ab} \mp \frac{q_a q_b q_c}{2} \partial_{k_a} \mathcal{G}_s^{bc}. \quad (4)$$

Here, $\mathcal{G}_s^{ab}(\mathbf{k}) = [\text{Re} \langle \partial_{k_a} u_{s,\mathbf{k}} | \partial_{k_b} u_{s,\mathbf{k}} \rangle - \xi^a \xi^b]$ represents intraband quantum metric (or the Fubini-Study metric), with $\xi^a = i \langle u_{s,\mathbf{k}} | \partial_{k_a} u_{s,\mathbf{k}} \rangle$ being the single band Berry connection [13, 25, 41, 42], and a, b, c denote cartesian directions. The quantum metric measures the distance between two infinitesimally close Bloch states in Hilbert space as [42, 43] $D_{\mathbf{k},\mathbf{k}+d\mathbf{k}}^2 = 1 - |\langle u_{s,\mathbf{k}} | u_{s,\mathbf{k}+d\mathbf{k}} \rangle|^2 \simeq \mathcal{G}_s^{ab}(\mathbf{k}) d\mathbf{k}^a d\mathbf{k}^b$.

We work in the dynamical long-wavelength limit, $qv_F < \omega \ll \mu$ (v_F denotes Fermi-velocity) to probe long-wavelength plasmons. In this limit, we expand the real part of the density-density response function in different orders of $1/\omega$. The calculation details are discussed in Sec. S2 of SM. We obtain,

$$\text{Re} [\Pi_{\text{intra}}(\mathbf{q}, \omega)] = q_a q_b q_c \frac{Q_{abc}^{\mathbf{u}}}{\omega} + q_a q_b \frac{\mathcal{D}_{ab}^{\mathbf{u}}}{\omega^2} + q_a q_b q_c \frac{C_{abc}^{\mathbf{u}}}{\omega^3} + \dots \quad (5)$$

We have used the \mathbf{u} -superscript to denote their drift current dependence. The expansion coefficients of Eq. 5 are specified by,

$$Q_{abc}^{\mathbf{u}} = -g_s \sum_{s,\mathbf{k}} \tilde{f}_{s,\mathbf{k}} \partial_{k_a} \mathcal{G}_s^{bc}(\mathbf{k}), \quad (6)$$

$$\mathcal{D}_{ab}^{\mathbf{u}} = g_s \sum_{s,\mathbf{k}} \tilde{f}_{s,\mathbf{k}} \left(\frac{\partial^2 E_{s,\mathbf{k}}}{\partial k_a \partial k_b} \right), \quad (7)$$

$$C_{abc}^{\mathbf{u}} = 2g_s \sum_{s,\mathbf{k}} \tilde{f}_{s,\mathbf{k}} \left(v_{s,\mathbf{k}}^a \frac{\partial^2 E_{s,\mathbf{k}}}{\partial k_b \partial k_c} \right). \quad (8)$$

Here, $v_{s,\mathbf{k}}^a = \partial E_{s,\mathbf{k}} / \partial k_a$ represents the band velocity component. $Q_{abc}^{\mathbf{u}}$ is the drift-induced quantum-metric dipole [13, 26, 41, 44]. It is analogous to the Berry curvature dipole [45], with the Berry curvature [45] substituted by the quantum metric. In Eq. (7), $\mathcal{D}_{ab}^{\mathbf{u}}$ is the drift-renormalized Drude-weight. In Eq. (8), $C_{abc}^{\mathbf{u}}$ arises from the polarization of the Fermi-surface due to the momentum shift ($\delta_{\mathbf{k}}$) induced by the DC bias.

We find that the odd $1/\omega$ expansion coefficients in Eq. (6) and Eq. (8) are crucial for supporting nonreciprocal plasmons in the systems with $\Pi(\mathbf{q}, \omega) \neq \Pi(-\mathbf{q}, \omega)$. In the absence of drift, $Q_{abc}^{\mathbf{u}}$ and $C_{abc}^{\mathbf{u}}$ will be identically zero unless the system intrinsically breaks the inversion and time-reversal symmetry, simultaneously [13, 15]. In that case, $Q_{abc}^{\mathbf{u}=0}$ and $C_{abc}^{\mathbf{u}=0}$ give rise to intrinsic nonreciprocal plasmon modes in noncentrosymmetric magnetic systems [13, 15]. However, the unidirectional flow

of drifting electrons breaks both the time-reversal and inversion symmetry, and it leads to an asymmetric Fermi-distribution function, $\tilde{f}_{s,\mathbf{k}} \neq \tilde{f}_{s,-\mathbf{k}}$. Therefore, the \mathbf{k} -integration of Eq. (6), and Eq. (8) are non-zero, yielding finite values of $\mathcal{Q}_{abc}^{\mathbf{u}}$ and $\mathcal{C}_{abc}^{\mathbf{u}}$ in presence of finite u in all quantum systems.

We obtain the plasmon frequency by solving for the roots of Eq. (1) on the real axis [30], assuming the Landau damping to be relatively small. Retaining terms up to ω^3 in Eq. (5), we can approximate the long wavelength nonreciprocal plasmon dispersion. We calculate the drift-induced nonreciprocal plasmon dispersion for small q , up to linear order in u , to be (see Sec. S3 of SM for details)

$$\omega_p^{\mathbf{u}}(\mathbf{q}) \approx \sqrt{q^2 V_q \mathcal{D}^{\mathbf{u}}} + \Delta\omega_p^{\mathcal{C}} + \Delta\omega_p^{\mathcal{Q}}. \quad (9)$$

Here, $\Delta\omega_p^{\mathcal{C}} = q\mathcal{C}^{\mathbf{u}}/2\mathcal{D}^{\mathbf{u}}$ captures the classical plasmon Doppler shift, and $\Delta\omega_p^{\mathcal{Q}} = q^3 V_q \mathcal{Q}^{\mathbf{u}}/2$ is the quantum plasmon Doppler shift.

Equation (9) captures the long-wavelength limit of nonreciprocal plasmon dispersion for general quantum systems with a DC current (retaining terms up to linear order in \mathbf{u}). Here, the first term captures the reciprocal plasmon dispersion with a drift velocity modified Drude weight, $\mathcal{D}^0 \rightarrow \mathcal{D}^{\mathbf{u}}$. Both of the other terms capture the nonreciprocal dispersion, as the sign of $\mathcal{Q}^{\mathbf{u}}$, and $\mathcal{C}^{\mathbf{u}}$ depends on whether the plasmon propagates along or opposite to the drift flow, *i.e.*, $\hat{\mathbf{q}} \cdot \hat{\mathbf{u}} = \pm 1$. Of these two, the $\Delta\omega_p^{\mathcal{C}}$ term is a linear-in- q correction while the $\Delta\omega_p^{\mathcal{Q}}$ captures a quadratic correction to the nonreciprocal plasmon dispersion (for unscreened Coulomb interactions). The frequency shift $\Delta\omega_p^{\mathcal{C}}$ arises from the drift velocity induced shift of the Fermi-surface, and it is typically referred to as classical correction or classical plasmonic Doppler shift [46]. In contrast, the second correction term, $\Delta\omega_p^{\mathcal{Q}}$ in Eq. (9) has a completely quantum origin associated with the quantum-metric dipole, $\mathcal{Q}^{\mathbf{u}}$. We term this correction as quantum plasmonic Doppler shift, as it arises from the nontrivial quantum geometry of the Bloch state [47]. This additional correction to the Doppler shift is one of the main findings of this manuscript. Interestingly, the quantum correction to the plasmonic Doppler shift can also be derived from a semiclassical hydrodynamic description. We present the semiclassical description of the plasmonic Doppler shift in Sec. 4 of SM.

To quantify the classical and quantum nonreciprocity, we compute the percentage of nonreciprocity,

$$\frac{|\omega_p^{\mathbf{u}}(\mathbf{q}) - \omega_p^{\mathbf{u}}(-\mathbf{q})|}{\omega_p^0(\mathbf{q})} = \underbrace{\sqrt{q} \frac{\mathcal{C}^{\mathbf{u}}}{\mathcal{D}^{\mathbf{u}}} \sqrt{\frac{\kappa}{2\pi e^2 \mathcal{D}^0}}}_{\eta^{\mathcal{C}}} + \underbrace{q^{3/2} \mathcal{Q}^{\mathbf{u}} \sqrt{\frac{2\pi e^2}{\kappa \mathcal{D}^0}}}_{\eta^{\mathcal{Q}}}. \quad (10)$$

Here, $\eta^{\mathcal{C}}$ and $\eta^{\mathcal{Q}}$ denote the percentage of classical and quantum plasmonic nonreciprocity, respectively, and we have defined $\mathcal{D}^0 \equiv \mathcal{D}^{\mathbf{u}=0}$. Having established the origin of drift-induced quantum nonreciprocity, we next explore

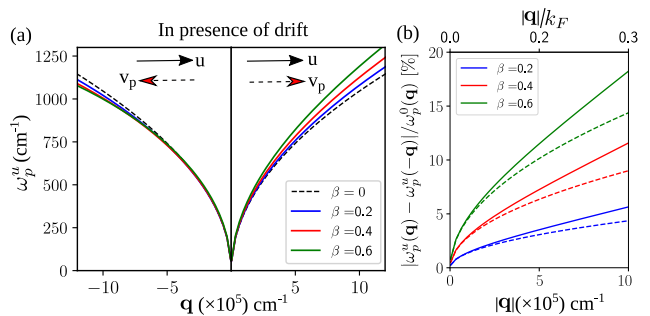


FIG. 2. (a) Plasmon dispersion for current-carrying graphene under different carrier drift velocities, $\beta = u/v_F = 0.2, 0.4, \text{ and } 0.6$, respectively. Here, $v_p = d\omega_p/dq$ indicates the group velocity of plasmons. We have used $\alpha_{ee} = 0.9$ for air/SLG/SiO₂ interface [48] and carrier density, $n = 2.9 \times 10^{12} \text{ cm}^{-2}$ [16]. (b) Total percentage of nonreciprocity, $|\omega_p^{\mathbf{u}}(\mathbf{q}) - \omega_p^{\mathbf{u}}(-\mathbf{q})|/\omega_p^0(\mathbf{q})$ as a function of momentum (\mathbf{q}) for current-carrying graphene with different β . The dashed line represents the classical percentage of nonreciprocity ($\eta^{\mathcal{C}}$) as defined in Eq. (15). The horizontal q -axis has been scaled in terms of the Fermi wavevector (k_F) at the top of the panel (b). For SLG, the percentage of nonreciprocity is mainly dominated by classical contribution $\Delta\omega_p^{\mathcal{C}}$.

the magnitude of these terms in two-dimensional electron gas (2DEG), graphene, and twisted bilayer graphene.

III. Quantum nonreciprocity in graphene and 2DEG

We calculate Eq. (9) for 2DEG with parabolic dispersion and graphene having linear dispersion to elucidate classical and quantum nonreciprocity. The wavefunction of a 2DEG is a single component object, and as a consequence, the band overlap term $F_{\mathbf{k},\mathbf{k}\pm\mathbf{q}} = 1$. This can also be seen from the fact that the Berry curvature and quantum metric vanish in single-component systems. Thus, a 2DEG can only support classical nonreciprocity with $\Delta\omega_p^{\mathcal{C}} = \mathbf{u} \cdot \mathbf{q}$, and the quantum contribution vanishes completely. We obtain the drift-induced plasmon dispersion for 2DEG from Eq. (9) to be,

$$\omega_{2\text{DEG}}^{\mathbf{u}}(\mathbf{q}) \approx \sqrt{\frac{2\pi n e^2}{\kappa m} q} + \mathbf{u} \cdot \mathbf{q}. \quad (11)$$

Here, n is the 2DEG carrier density and m is the effective mass. The detailed derivations are shown in Sec. S5 of SM [38].

In contrast to 2DEG, the low energy electronic states for graphene is represented by 2D massless Dirac Hamiltonian, specified by $\mathcal{H}_{\mathbf{k}} = v_F \sigma \cdot \mathbf{k}$ with $\sigma = (\sigma_x, \sigma_y)$ being the vector of the Pauli matrices and v_F is the Fermi velocity [49]. This Hamiltonian has two component spinor eigenstates, $|\mathbf{k}, s\rangle = (1/\sqrt{2}) (e^{-i\theta} \ s)^T$, with eigenvalues, $E_{s,\mathbf{k}} = s v_F |\mathbf{k}|$ for conduction ($s = 1$) and valence ($s = -1$) band respectively, and $\theta = \tan^{-1}(k_y/k_x)$.

To understand the role of quantum geometry, we calculate band resolved quantum metric, and it is given by $\mathcal{G}_+^{xx}(\mathbf{k}) = \mathcal{G}_-^{xx}(\mathbf{k}) = \sin^2 \theta / (4k^2)$. The corresponding band overlap term can be evaluated using Eq. (4). For $\mathbf{q} = q\hat{\mathbf{x}}$, it is given by

$$F_{\mathbf{k}\pm\mathbf{q},\mathbf{k}}^{++} \approx 1 - \frac{q^2}{4k^2} \sin^2 \theta \pm \cos \theta \sin^2 \theta \frac{q^3}{2k^3}. \quad (12)$$

To include the impact of the unidirectional drift flow $\mathbf{u} = u\hat{\mathbf{x}}$ in the Fermi-Dirac distribution, we model it for $T = 0$ as $\tilde{f}_{+,\mathbf{k}} = \Theta[k_F(\theta) - k]$, where $k_F(\theta) = k_F/[1 - \beta \cos(\theta - \phi_u)]$. Here, $\beta = u/v_F$, and ϕ_u is the angle between \mathbf{u} and plasmon wavevector \mathbf{q} . With this modified Fermi-distribution function, we can calculate the quantum metric dipole to be $\mathcal{Q}^{\mathbf{u}} = \gamma g_s u / (16\pi|\mu|)$. Here, $g_s = 4$ represent total spin and valley degeneracy, μ is the chemical potential, and $\gamma = \hat{\mathbf{q}} \cdot \hat{\mathbf{u}}$. For example, $\gamma = +1$ (-1) represents an up-stream (down-stream) plasmon propagation with respect to the drift of the charge carriers. We calculate the other expansion coefficients of $\Pi(\mathbf{q}, \omega)$ in Eq. (5) to be,

$$\mathcal{D}^{\mathbf{u}} = \frac{g_s |\mu| W(\beta)}{4\pi \beta}, \quad C^{\mathbf{u}} = \gamma \frac{g_s v_F |\mu| W(\beta)^2}{8\pi \beta}. \quad (13)$$

Here, we have defined $W(\beta) = 2(1 - \sqrt{1 - \beta^2})/\beta$ and this relativistic factor becomes unity as $u \rightarrow 0$, or $\lim_{\beta \rightarrow 0} W(\beta)/\beta = 1$ [21]. Combining these terms, we calculate the long wavelength drift-induced nonreciprocal plasmon dispersion for graphene to be (see Sec. S6 of SM [38] for detailed calculations),

$$\begin{aligned} \omega_p^{\mathbf{u}}(\mathbf{q}) \approx & \sqrt{\frac{2D_0 W(\beta)}{\kappa\beta}} \sqrt{q} \left[1 + \frac{12 - 16\alpha_{ee}^2}{16} \frac{q}{k_{\text{TF}}} \right] \\ & + \gamma \frac{W(\beta)}{4\beta} u q + \gamma \frac{\alpha_{ee}}{4k_F} u q^2. \end{aligned} \quad (14)$$

Here, $D_0 = e^2 \mu / \hbar^2$ is the non-interacting Drude-weight at $T = 0$ for the 2D massless Dirac Hamiltonian [48], $\alpha_{ee} = e^2 / (\kappa \hbar v_F)$ is the effective-fine structure constant, and $k_{\text{TF}} = 4\alpha_{ee} k_F$ and κ is the background dielectric constant. In Eq. (14), the last two nonreciprocal terms are calculated up to linear order in the drift velocity [16, 21].

In Eq. (14), the classical Doppler shift due to $C^{\mathbf{u}}$ is $\Delta\omega_p^{\mathcal{C}} = \gamma[W(\beta)/4\beta]uq$, which arises from the polarization of Fermi surface under DC field. Additionally, there is a quantum correction in Eq. (14) originating from the quantum-metric dipole $\mathcal{Q}^{\mathbf{u}}$, and this quantum Doppler shift is given by $\Delta\omega_p^{\mathcal{Q}} = \gamma(\alpha_{ee}/4k_F)uq^2$. This quantum correction goes as q^2 and varies with the carrier density as $n^{-1/2}$. We calculate the classical and quantum percentage of nonreciprocity in the plasmon dispersion to be,

$$\eta^{\mathcal{C}} \equiv \frac{\Delta\omega_p^{\mathcal{C}}(q)}{\omega_p^0(q)} \sim \frac{1}{\alpha_{ee}} \frac{W(\beta)}{4\beta} \frac{u}{v_F} \frac{\omega_p^0(q)}{|\mu|}, \quad (15)$$

$$\eta^{\mathcal{Q}} \equiv \frac{\Delta\omega_p^{\mathcal{Q}}(q)}{\omega_p^0(q)} \sim \frac{u}{v_F} \frac{\omega_p^0(q)}{4|\mu|} \frac{q}{k_F}. \quad (16)$$

Graphene	$\eta^{\mathcal{C}} = \frac{\Delta\omega_p^{\mathcal{C}}(q)}{\omega_p^0(q)}$	$\eta^{\mathcal{Q}} = \frac{\Delta\omega_p^{\mathcal{Q}}(q)}{\omega_p^0(q)}$
wavevector	$q^{1/2}$	$q^{3/2}$
Carrier density	$n^{-1/4}$	$n^{-3/4}$
Effective fine structure (α_{ee})	$\alpha_{ee}^{-1/2}$	$\alpha_{ee}^{1/2}$

TABLE I. The dependence of classical ($\eta^{\mathcal{C}}$) and quantum ($\eta^{\mathcal{Q}}$) percentage of plasmonic nonreciprocity for graphene on the wavevector, carrier density, and the effective-fine structure constant.

Here, $\omega_p^0(q) = |\mu| \sqrt{2\alpha_{ee}} (q/k_F)^{1/2}$ is the long-wavelength plasmon dispersion for graphene without drift flow [50]. We compare the dependence of both these corrections on different parameters such as wavevector, carrier density, and the interaction strength in Table I. We find that the quantum correction to the nonreciprocity is more sensitive to all these parameters.

In Fig. 2(a), we present the total nonreciprocal plasmon dispersion in graphene for different drift velocities or β . This includes both classical and quantum corrections. We also show the classical and total percentage of nonreciprocity separately in Fig. 2 (b). For graphene, the total percentage of nonreciprocity is mainly dictated by the classical contribution with $\eta^{\mathcal{C}}$ [16]. The quantum correction is small in the range of experimentally accessible wavevectors. This is because the quantum correction $\Delta\omega_p^{\mathcal{Q}} \sim \alpha_{ee} u q^2$ is smaller for small wavevectors ($q < k_F$) with $\alpha_{ee} \approx 1$ [48]. The quantum correction can become significant for a larger wavevector ($q > k_F$), but the plasmon enters the particle-hole continuum region and becomes Landau damped [50]. This suggests that the quantum nonreciprocity of the plasmon dispersion can become larger in moiré superlattices of graphene, which support more significant $\alpha_{ee} \gg 1$ [19], and long-lived plasmon for larger wavevectors. Motivated by this, we investigate drift-induced nonreciprocal plasmon dispersion in the moiré superlattice of twisted-bilayer graphene in the next section.

IV. Large plasmonic nonreciprocity in twisted bilayer graphene

Moiré superlattices, in general, and TBG, in particular, have attracted a lot of attention in near-field optical spectroscopy studies for probing novel collective plasmon modes [14, 29, 52]. Here, we specifically focus on the nature of drift-induced nonreciprocal plasmon in *magic* angle TBG.

The moiré superlattice has a large periodicity, of the order of tens of nanometers, for a small twist angle (θ). The real space lattice constant is specified by $L_M = a/[2\sin(\theta/2)]$, where $a \approx 0.246$ nm. This also leads to a smaller moiré Brillouin zone, with a reciprocal lattice vector of magnitude $k_M = k_{\text{BG}} \sin(\theta/2)$, with k_{BG} de-

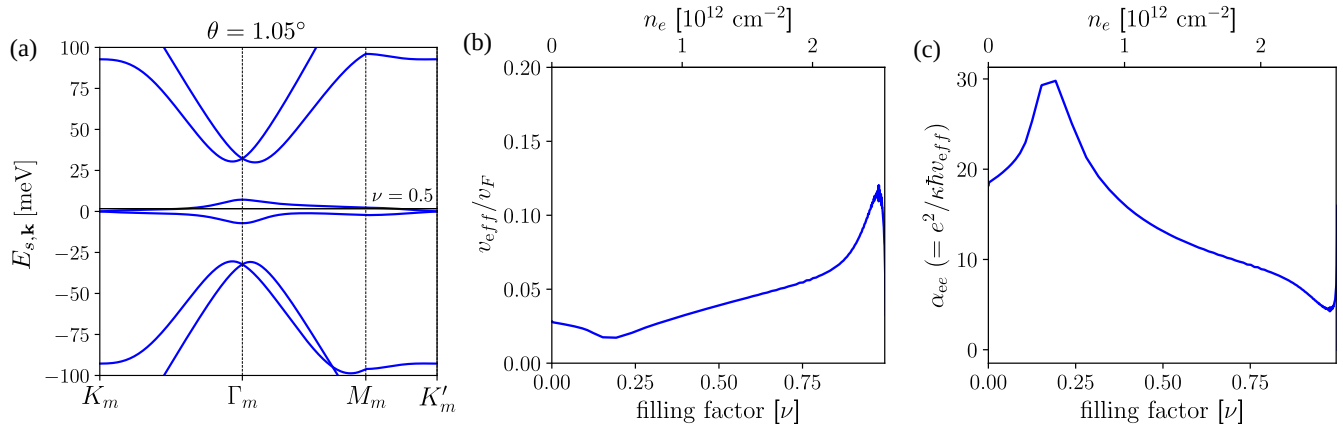


FIG. 3. (a) Band dispersion of twisted-bilayer graphene near magic angle $\theta = 1.05^\circ$ for K-valley only. We have used $u_0 = 79.7$ meV and $u_1 = 97.5$ meV in the continuum model [51]. The chemical potential is set at $\mu = 1.65$ meV, corresponding to half-filling. (b) The variation of effective Fermi-velocity (v_{eff}) of TBG with charge filling factor, ν in terms of Dirac fermion velocity ($v_F \approx 0.87 \times 10^6$ m/s) of single-layer graphene. Here, n_e denotes the corresponding carrier density. (c) Variation of the effective fine structure constant, α_{ee} for twisted bilayer graphene with filling factor. $\alpha_{ee} > 10$ for a significant region of the band occupancy.

noting the magnitude of the reciprocal lattice for bilayer-graphene (BG). Due to the interlayer electronic coupling and modulation of Dirac fermions by moiré superlattice potentials [51, 53], the electronic band dispersion of small angle TBG shows distinct features compared to SLG and Bernal-stacked BG. Near magic angle $\theta \approx 1.05^\circ$, the low energy band structure of TBG has four quasi-flat bands (two for valley, and two for spin degeneracy) with minimal bandwidth (~ 8 meV) as shown in Fig. 3(a). The description of the continuum model Hamiltonian is discussed in Sec. S7 of SM [38, 54–58]. As a consequence, the effective Fermi velocity (v_{eff}) of the carriers close to the charge neutrality point becomes around $v_{\text{eff}} \sim 0.04v_F$, while SLG has $v_F = 0.86 \times 10^6$ m/s [see Fig. 3(b)]. As a consequence, the effective fine-structure constant in TBG, $\alpha_{ee} = e^2/(\kappa\hbar v_{\text{eff}})$, gets significantly enhanced ($\alpha_{ee} \sim 20 - 30$) compared to SLG having $\alpha_{ee} \approx 1$ [48]. We highlight this explicitly in Fig. 3(c), by showing the variation of α_{ee} in the first conduction band with doping.

To demonstrate the nonreciprocal plasmons in TBG, we have numerically calculated the loss-function spectrum, $L(\mathbf{q}, \omega) = \text{Im}[-\epsilon^{-1}(\mathbf{q}, \omega)]$ including all the intra ($s = s'$) and interband ($s \neq s'$) transitions for both K and K' valley. We present the calculated loss-function spectrum in pristine TBG (without drifting carriers) in Fig. 4(a, b). For our calculations, we have used 2D Coulomb potential $V_q = 2\pi e^2/(\kappa|q|)$, with $\kappa = 4.9$ as the background static dielectric constant for hBN [59], and $T = 5$ K. The loss function displays sharp peaks at the plasmon poles and shows the long-lived nature of the intraband plasmons in TBG in the terahertz frequency regime. In contrast to plasmons in SLG, the intraband plasmon mode in TBG lies above the Pauli blocking regions [$\omega_p^0(q) \gg 2\mu$] [29]. It becomes undamped from particle-hole excitations for large momentum as shown

in Fig. 4(a). On applying a finite DC bias voltage and enabling drifting charge carriers in TBG, the Fermi surface shifts by momentum $\delta_{\mathbf{k}} = -\beta k_F^{\text{eff}} \hat{\mathbf{u}}$ where $\beta = u/v_{\text{eff}}$, and $v_{\text{eff}} = k_F^{\text{eff}}/m_{\text{eff}}$. Here, v_{eff} is the effective Fermi velocity, m_{eff} denotes the effective mass of the carriers, and $k_F^{\text{eff}} = \mu/(\hbar v_{\text{eff}})$ is the effective Fermi wavevector for TBG. We present the drift current (along x-direction) induced nonreciprocal loss function in the $\mathbf{q} - \omega$ plane in Fig. 4(b). The nonreciprocal nature of the plasmon dispersion with $\omega_p^{\mathbf{u}}(-\mathbf{q}) \neq \omega_p^{\mathbf{u}}(\mathbf{q})$ can be clearly seen. To investigate the classical correction in the nonreciprocity, we have calculated nonreciprocal dispersion in Fig. 4(c) by artificially setting the band-overlap factor, $F_{\mathbf{k}, \mathbf{k}+\mathbf{q}}^{ss'} = \delta_{ss'}$, where $\delta_{ss'}$ denotes Kronecker delta function. This approximation necessarily neglects all interband overlap terms, as well as band geometric corrections in TBG, mapping the TBG problem to a 2DEG case. The quantum corrections arise primarily from the quantum metric [see Eq. (6)], which dominates at larger wavevectors. This is because the plasmon mode is undamped in TBG for larger wavevectors, which allows to dominate $\Delta\omega_p^{\mathbf{Q}}(\mathbf{q})$ over $\Delta\omega_p^{\mathbf{C}}(\mathbf{q})$. We present the distribution of the quantum metric in the 2D Brillouin zone in Fig. 4(d).

Finally, we present the drift velocity dependence of the plasmon dispersion in Fig. 4(e) by numerically solving Eq. (1) for different ($\beta = u/v_{\text{eff}}$) values. We show the corresponding drift velocity dependence of the percentage of the plasmon nonreciprocity in Fig. 4(f). The classical correction overestimates the nonreciprocity for small q values. Interestingly, we find a significant increase in the percentage of total nonreciprocity between two oppositely propagating plasmon modes at larger wavevectors, driven predominantly by the quantum corrections [see Fig. 4(c)]. The quantum Doppler shift-induced plasmonic nonreciprocity can be more than 20% for $\beta \approx 0.6$.

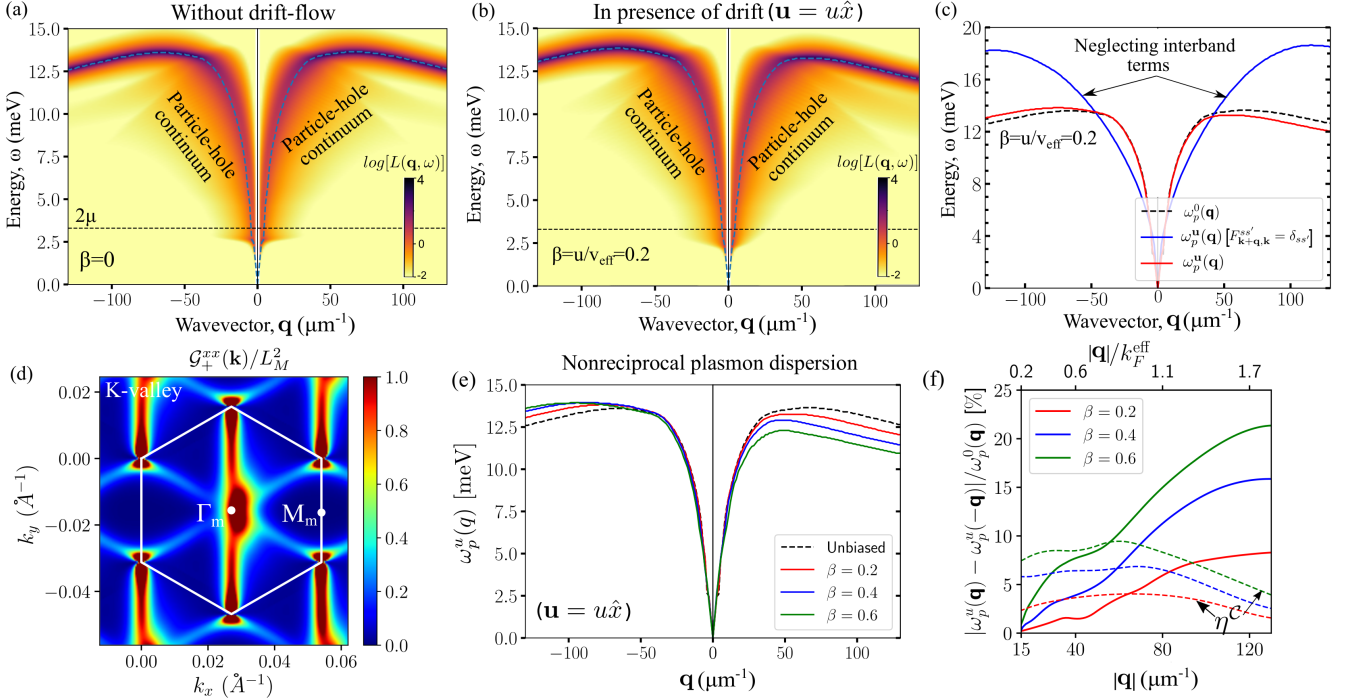


FIG. 4. (a) Colorplot of the loss function spectrum, $L(\mathbf{q}, \omega) = \text{Im}[-\epsilon^{-1}(\mathbf{q}, \omega)]$ in log scale for twisted bilayer graphene (TBG) encapsulated in hBN (with $\kappa = 4.9$ [59]) at half-filling ($\mu = 1.65$ meV) without any DC bias. We set wavevector $\mathbf{q} \parallel \Gamma_m$ - M_m direction as shown in panel (d). The cyan dashed line represents numerically evaluated plasmon dispersion by finding the roots of the dielectric function. (b) Loss function spectrum of biased TBG in the presence carriers drifting with velocity \mathbf{u} along the x-direction. The plasmon dispersion exhibits asymmetry for $+\mathbf{q}$ and $-\mathbf{q}$ wavevector. (c) Nonreciprocal plasmon dispersion (shown by blue line) in TBG, without considering band geometric corrections by setting $F_{\mathbf{k}+\mathbf{q}, \mathbf{k}}^{ss'} = \delta_{ss'}$. This neglects all interband contributions in the density-density response function. (d) Colormap of the quantum metric, $\mathcal{G}_+^{xx}(\mathbf{k})$ for the first conduction band in the K-valley. (e) Nonreciprocal plasmon dispersion in TBG for different values of $\beta = u/v_{\text{eff}} = 0.2, 0.4,$ and $0.6,$ respectively. (f) Total percentage of nonreciprocity (solid lines) in TBG with different β . The horizontal axis at the top of the panel has been scaled in terms of the effective Fermi wavevector $k_F^{\text{eff}} \approx 71 \mu\text{m}^{-1}$. The dashed lines represent the classical percentage of nonreciprocity (η^c) with band-overlap factor, $F_{\mathbf{k}, \mathbf{k} \pm \mathbf{q}}^{ss'} = \delta_{ss'}$. Here, quantum corrections dominate over classical contributions, particularly in large wavevectors.

Furthermore, given the low value of v_{eff} in TBG and in other moiré materials in general, achieving a more significant value of β in experiments should be feasible [60].

Our calculations strongly suggest that TBG and other moiré platforms with relatively flat bands can be good candidates to observe a significant quantum plasmonic Doppler effect. This is enabled by a rather large value of the effective interaction parameter ($\alpha_{ee} \propto 1/v_{\text{eff}}$) originating from the smaller band velocities in flat bands. It will be interesting to probe this large nonreciprocity in near-field imaging experiments [16, 52]. Further, we note that all our calculations are within the RPA, which misses out on exchange and correlation effect [30]. Generally, RPA works very well for the plasmon dispersion. In fact, the plasmonic Doppler shift, calculated within RPA, explains the experimental dispersion for single-layer graphene reasonably well [17]. However, subtle effects in the plasmon nonreciprocity induced by exchange and correlation effects cannot be ruled out completely.

V. Conclusion

In summary, our investigation into drift-induced nonreciprocal plasmon dispersion in a general quantum system has unveiled an intriguing quantum plasmonic nonreciprocity alongside the well-established classical Doppler shift. The classical correction ($\Delta\omega_p^c$) mainly arises from Fermi surface polarization under a DC electric field. In contrast, the quantum correction, ($\Delta\omega_p^q$), stems from the quantum-metric dipole - a fundamental band geometric property of the Bloch wave function.

Explicitly examining single-layer graphene and the moiré superlattice of twisted bilayer graphene, we observed distinct behaviors. In single-layer graphene, the classical term ($\Delta\omega_p^c \sim uq$) predominantly governs the plasmonic Doppler shift, with the quantum correction ($\Delta\omega_p^q \sim \alpha_{ee}uq^2$) being relatively smaller owing to its q^2 behavior with $\alpha_{ee} \approx 1$ [48]. Conversely, the quantum metric-induced plasmonic quantum Doppler shift takes precedence in twisted bilayer graphene. This dom-

inance arises from a small band velocity in the flat bands, resulting in a large effective fine structure constant ($\alpha_{ee} \approx 20 - 30$). Additionally, plasmons in twisted bilayer graphene remain practically undamped even for large values of q/k_F^{eff} , allowing the $\alpha_{ee}uq^2$ term in $\Delta\omega_p^{\mathcal{Q}}$ to influence the dispersion. Consequently, twisted bilayer graphene and other moiré systems can exhibit a plasmonic nonreciprocity of 20% or higher for reasonable drift velocities [60].

This exploration of drift-induced nonreciprocal plasmons in twisted bilayer graphene advances the fundamental understanding of the subject and paves the way for novel optoelectronic applications. Possibilities include the development of plasmonic isolators [61], one-

way waveguides [62], and optical transmission [63].

Acknowledgment

DD acknowledges the Indian Institute of Technology, Kanpur, for financial support. A. A acknowledges the Department of Science and Technology for Project No. DST/NM/TUE/QM-6/2019(G)-IIT Kanpur, of the Government of India, for financial support. We thank Atasi Chakraborty and Debottam Mandal for the valuable discussions. We acknowledge the high-performance computing facility at IIT Kanpur for computational support. We also acknowledge the National Supercomputing Mission (NSM) for providing computing resources for 'PARAM Sanganak' at IIT Kanpur.

-
- [1] Christophe Caloz, Andrea Alù, Sergei Tretyakov, Dimitrios Sounas, Karim Achouri, and Zoé-Lise Deck-Léger, “Electromagnetic nonreciprocity,” *Phys. Rev. Appl.* **10**, 047001 (2018).
- [2] R. J. Potton, “Reciprocity in optics,” *Reports on Progress in Physics* **67**, 717 (2004).
- [3] Svetlana V. Boriskina, Morgan Blevins, and Simo Pajovic, “The nonreciprocal adventures of light,” *Opt. Photon. News* **33**, 46–53 (2022).
- [4] Yoshinori Tokura and Naoto Nagaosa, “Nonreciprocal responses from non-centrosymmetric quantum materials,” *Nature Communications* **9**, 3740 (2018).
- [5] Lei Bi, Juejun Hu, Peng Jiang, Dong Hun Kim, Gerald F. Dionne, Lionel C. Kimerling, and C. A. Ross, “On-chip optical isolation in monolithically integrated non-reciprocal optical resonators,” *Nature Photonics* **5**, 758–762 (2011).
- [6] K. L. Tsakmakidis, L. Shen, S. A. Schulz, X. Zheng, J. Upham, X. Deng, H. Altug, A. F. Vakakis, and R. W. Boyd, “Breaking lorentz reciprocity to overcome the time-bandwidth limit in physics and engineering,” *Science* **356**, 1260–1264 (2017).
- [7] Francesco Monticone, “A truly one-way lane for surface plasmon polaritons,” *Nature Photonics* **14**, 461–465 (2020).
- [8] S. Ali Hassani Gangaraj and Francesco Monticone, “Drifting electrons: Nonreciprocal plasmonics and thermal photonics,” *ACS Photonics* **9**, 806–819 (2022).
- [9] D. N. Basov, M. M. Fogler, and F. J. García de Abajo, “Polaritons in van der waals materials,” *Science* **354**, aag1992 (2016).
- [10] Antoine Reserbat-Plantey, Itai Epstein, Iacopo Torre, Antonio T. Costa, P. A. D. Gonçalves, N. Asger Mortensen, Marco Polini, Justin C. W. Song, Nuno M. R. Peres, and Frank H. L. Koppens, “Quantum nanophotonics in two-dimensional materials,” *ACS Photonics* **8**, 85–101 (2021).
- [11] Carlo Rizza, Debasis Dutta, Barun Ghosh, Francesca Alessandro, Chia-Nung Kuo, Chin Shan Lue, Lorenzo S. Caputi, Arun Bansil, Vincenzo Galdi, Amit Agarwal, Antonio Politano, and Anna Cupolillo, “Extreme optical anisotropy in the type-ii dirac semimetal nite2 for applications to nanophotonics,” *ACS Applied Nano Materials* (2022), 10.1021/acsnm.2c04340.
- [12] Justin C. W. Song and Mark S. Rudner, “Chiral plasmons without magnetic field,” *Proceedings of the National Academy of Sciences* **113**, 4658–4663 (2016).
- [13] Arpit Arora, Mark S. Rudner, and Justin C. W. Song, “Quantum plasmonic nonreciprocity in parity-violating magnets,” *Nano Letters* **22**, 9351–9357 (2022).
- [14] Tianye Huang, Xuecou Tu, Changqing Shen, Binjie Zheng, Junzhan Wang, Hao Wang, Kaveh Khaliji, Sang Hyun Park, Zhiyong Liu, Teng Yang, Zhidong Zhang, Lei Shao, Xuesong Li, Tony Low, Yi Shi, and Xiaomu Wang, “Observation of chiral and slow plasmons in twisted bilayer graphene,” *Nature* **605**, 63–68 (2022).
- [15] Debasis Dutta, Atasi Chakraborty, and Amit Agarwal, “Intrinsic nonreciprocal bulk plasmons in noncentrosymmetric magnetic systems,” *Phys. Rev. B* **107**, 165404 (2023).
- [16] Y. Dong, L. Xiong, I. Y. Phinney, Z. Sun, R. Jing, A. S. McLeod, S. Zhang, S. Liu, F. L. Ruta, H. Gao, Z. Dong, R. Pan, J. H. Edgar, P. Jarillo-Herrero, L. S. Levitov, A. J. Millis, M. M. Fogler, D. A. Bandurin, and D. N. Basov, “Fizeau drag in graphene plasmonics,” *Nature* **594**, 513–516 (2021).
- [17] Wenyu Zhao, Sihan Zhao, Hongyuan Li, Sheng Wang, Shaoxin Wang, M. Iqbal Bakti Utama, Salman Kahn, Yue Jiang, Xiao Xiao, SeokJae Yoo, Kenji Watanabe, Takashi Taniguchi, Alex Zettl, and Feng Wang, “Efficient fizeau drag from dirac electrons in monolayer graphene,” *Nature* **594**, 517–521 (2021).
- [18] Dan S. Borgnia, Trung V. Phan, and Leonid S. Levitov, “Quasi-relativistic doppler effect and non-reciprocal plasmons in graphene,” (2015).
- [19] Michał Papaj and Cyprian Lewandowski, “Plasmonic nonreciprocity driven by band hybridization in moiré materials,” *Phys. Rev. Lett.* **125**, 066801 (2020).
- [20] Tiago A. Morgado and Mário G. Silveirinha, “Directional dependence of the plasmonic gain and nonreciprocity in drift-current biased graphene,” *Nanophotonics* **11**, 4929–4936 (2022).
- [21] Ben Van Duppen, Andrea Tomadin, Alexander N Grigorenko, and Marco Polini, “Current-induced birefringent

- absorption and non-reciprocal plasmons in graphene,” *2D Materials* **3**, 015011 (2016).
- [22] Mohsen Sabbaghi, Hyun-Woo Lee, Tobias Stauber, and Kwang S. Kim, “Drift-induced modifications to the dynamical polarization of graphene,” *Phys. Rev. B* **92**, 195429 (2015).
- [23] Tiago A. Morgado and Mário G. Silveirinha, “Nonlocal effects and enhanced nonreciprocity in current-driven graphene systems,” *Phys. Rev. B* **102**, 075102 (2020).
- [24] Tiago A. Morgado and Mário G. Silveirinha, “Directional dependence of the plasmonic gain and nonreciprocity in drift-current biased graphene,” *Nanophotonics* **11**, 4929–4936 (2022).
- [25] J. P. Provost and G. Vallee, “Riemannian structure on manifolds of quantum states,” *Communications in Mathematical Physics* **76**, 289–301 (1980).
- [26] Anyuan Gao, Yu-Fei Liu, Jian-Xiang Qiu, Barun Ghosh, Thaís V. Trevisan, Yugo Onishi, Chaowei Hu, Tiema Qian, Hung-Ju Tien, Shao-Wen Chen, Mengqi Huang, Damien Bérubé, Houchen Li, Christian Tzschaschel, Thao Dinh, Zhe Sun, Sheng-Chin Ho, Shang-Wei Lien, Bahadur Singh, Kenji Watanabe, Takashi Taniguchi, David C. Bell, Hsin Lin, Tay-Rong Chang, Chunhui Rita Du, Arun Bansil, Liang Fu, Ni Ni, Peter P. Orth, Qiong Ma, and Su-Yang Xu, “Quantum metric nonlinear hall effect in a topological antiferromagnetic heterostructure,” *Science* **381**, 181–186 (2023).
- [27] Jie Wang, Jennifer Cano, Andrew J. Millis, Zhao Liu, and Bo Yang, “Exact landau level description of geometry and interaction in a flatband,” *Phys. Rev. Lett.* **127**, 246403 (2021).
- [28] Pankaj Bhalla, Kamal Das, Dimitrie Culcer, and Amit Agarwal, “Resonant second-harmonic generation as a probe of quantum geometry,” *Phys. Rev. Lett.* **129**, 227401 (2022).
- [29] Cyprian Lewandowski and Leonid Levitov, “Intrinsically undamped plasmon modes in narrow electron bands,” *Proceedings of the National Academy of Sciences* **116**, 20869–20874 (2019).
- [30] G. Giuliani and G. Vignale, *Quantum Theory of the Electron Liquid* (Cambridge University Press, 2005).
- [31] David Pines and J. Robert Schrieffer, “Approach to equilibrium of electrons, plasmons, and phonons in quantum and classical plasmas,” *Physical Review* **125**, 804–812 (1962).
- [32] Debasis Dutta, Barun Ghosh, Bahadur Singh, Hsin Lin, Antonio Politano, Arun Bansil, and Amit Agarwal, “Collective plasmonic modes in the chiral multifold fermionic material *coSi*,” *Phys. Rev. B* **105**, 165104 (2022).
- [33] Amit Agarwal, Marco Polini, Giovanni Vignale, and Michael E. Flatté, “Long-lived spin plasmons in a spin-polarized two-dimensional electron gas,” *Phys. Rev. B* **90**, 155409 (2014).
- [34] Amit Agarwal and Giovanni Vignale, “Plasmons in spin-polarized graphene: A way to measure spin polarization,” *Phys. Rev. B* **91**, 245407 (2015).
- [35] Rashmi Sachdeva, Anmol Thakur, Giovanni Vignale, and Amit Agarwal, “Plasmon modes of a massive dirac plasma, and their superlattices,” *Physical Review B* **91**, 205426 (2015).
- [36] R. Bistritzer and A. H. MacDonald, “Hydrodynamic theory of transport in doped graphene,” *Phys. Rev. B* **80**, 085109 (2009).
- [37] W. John, “V. f. gantmakher, y. b. levinson. carrier scattering in metals and semiconductors. modern problems in condensed matter sciences vol. 19. north-holland: Amsterdam, oxford, new york, tokyo 1987, 459 seiten. dfl. 280.00. isbn 0-444-87025-3,” *Crystal Research and Technology* **23**, 230–230 (1988).
- [38] The Supplemental material discusses, i) Eq. 2 in different regimes, ii) The density-density response function in small q limit, iii) Calculation of nonreciprocal plasmon dispersion, iv) Hydrodynamic theory of quantum plasmonic Doppler shift, v) Nonreciprocal plasmons in 2DEG, vi) Nonreciprocal plasmon dispersion in graphene, vii) Continuum model Hamiltonian for twisted bilayer graphene, viii) Effective Fermi velocity in twisted bilayer graphene.
- [39] Amit Agarwal, Stefano Chesi, T. Jungwirth, Jairo Sinova, G. Vignale, and Marco Polini, “Plasmon mass and drude weight in strongly spin-orbit-coupled two-dimensional electron gases,” *Phys. Rev. B* **83**, 115135 (2011).
- [40] Enrico Rossi, “Quantum metric and correlated states in two-dimensional systems,” *Current Opinion in Solid State and Materials Science* **25**, 100952 (2021).
- [41] Yang Gao and Di Xiao, “Nonreciprocal directional dichroism induced by the quantum metric dipole,” *Phys. Rev. Lett.* **122**, 227402 (2019).
- [42] R. Resta, “The insulating state of matter: a geometrical theory,” *The European Physical Journal B* **79**, 121–137 (2011).
- [43] Ahmed Abouelkomsan, Kang Yang, and Emil J. Bergholtz, “Quantum metric induced phases in moiré materials,” *Phys. Rev. Res.* **5**, L012015 (2023).
- [44] Matthew F. Lapa and Taylor L. Hughes, “Semiclassical wave packet dynamics in nonuniform electric fields,” *Phys. Rev. B* **99**, 121111 (2019).
- [45] Inti Sodemann and Liang Fu, “Quantum nonlinear hall effect induced by berry curvature dipole in time-reversal invariant materials,” *Phys. Rev. Lett.* **115**, 216806 (2015).
- [46] Haoyang Gao, Zhiyu Dong, and Leonid Levitov, “Plasmonic drag in a flowing fermi liquid,” (2019), [arXiv:1912.13409 \[cond-mat.mes-hall\]](https://arxiv.org/abs/1912.13409).
- [47] Di Xiao, Ming-Che Chang, and Qian Niu, “Berry phase effects on electronic properties,” *Rev. Mod. Phys.* **82**, 1959–2007 (2010).
- [48] A. N. Grigorenko, M. Polini, and K. S. Novoselov, “Graphene plasmonics,” *Nature Photonics* **6**, 749–758 (2012).
- [49] A. H. Castro Neto, F. Guinea, N. M. R. Peres, K. S. Novoselov, and A. K. Geim, “The electronic properties of graphene,” *Rev. Mod. Phys.* **81**, 109–162 (2009).
- [50] B Wunsch, T Stauber, F Sols, and F Guinea, “Dynamical polarization of graphene at finite doping,” *New Journal of Physics* **8**, 318–318 (2006).
- [51] Mikito Koshino, Noah F. Q. Yuan, Takashi Koretsune, Masayuki Ochi, Kazuhiko Kuroki, and Liang Fu, “Maximally localized wannier orbitals and the extended hubbard model for twisted bilayer graphene,” *Phys. Rev. X* **8**, 031087 (2018).
- [52] Niels C. H. Hesp, Iacopo Torre, Daniel Rodan-Legrain, Pietro Novelli, Yuan Cao, Stephen Carr, Shiang Fang, Petr Stepanov, David Barcons-Ruiz, Hanan Herzig Sheinfux, Kenji Watanabe, Takashi Taniguchi, Dmitri K. Efetov, Efthimios Kaxiras, Pablo Jarillo-Herrero, Marco

- Polini, and Frank H. L. Koppens, “Observation of interband collective excitations in twisted bilayer graphene,” *Nature Physics* **17**, 1162–1168 (2021).
- [53] Rafi Bistritzer and Allan H. MacDonald, “Moiré bands in twisted double-layer graphene,” *Proceedings of the National Academy of Sciences* **108**, 12233–12237 (2011).
- [54] Eva Y. Andrei and Allan H. MacDonald, “Graphene bilayers with a twist,” *Nature Materials* **19**, 1265–1275 (2020).
- [55] J. M. B. Lopes dos Santos, N. M. R. Peres, and A. H. Castro Neto, “Graphene bilayer with a twist: Electronic structure,” *Phys. Rev. Lett.* **99**, 256802 (2007).
- [56] Atasi Chakraborty, Debasis Dutta, and Amit Agarwal, “Tunable interband and intraband plasmons in twisted double bilayer graphene,” *Phys. Rev. B* **106**, 155422 (2022).
- [57] Subhajit Sinha, Pratap Chandra Adak, Atasi Chakraborty, Kamal Das, Koyendrila Debnath, L. D. Varma Sangani, Kenji Watanabe, Takashi Taniguchi, Umesh V. Waghmare, Amit Agarwal, and Mandar M. Deshmukh, “Berry curvature dipole senses topological transition in a moiré superlattice,” *Nature Physics* **18**, 765–770 (2022).
- [58] Atasi Chakraborty, Kamal Das, Subhajit Sinha, Pratap Chandra Adak, Mandar M Deshmukh, and Amit Agarwal, “Nonlinear anomalous hall effects probe topological phase-transitions in twisted double bilayer graphene,” *2D Materials* **9**, 045020 (2022).
- [59] Pietro Novelli, Iacopo Torre, Frank H. L. Koppens, Fabio Taddei, and Marco Polini, “Optical and plasmonic properties of twisted bilayer graphene: Impact of interlayer tunneling asymmetry and ground-state charge inhomogeneity,” *Physical Review B* **102**, 125403 (2020).
- [60] Alexey I. Berdyugin, Na Xin, Haoyang Gao, Sergey Slizovskiy, Zhiyu Dong, Shubhadeep Bhattacharjee, P. Kumaravadivel, Shuigang Xu, L. A. Ponomarenko, Matthew Holwill, D. A. Bandurin, Minsoo Kim, Yang Cao, M. T. Greenaway, K. S. Novoselov, I. V. Grigorieva, K. Watanabe, T. Taniguchi, V. I. Fal’ko, L. S. Levitov, Roshan Krishna Kumar, and A. K. Geim, “Out-of-equilibrium criticalities in graphene superlattices,” *Science* **375**, 430–433 (2022).
- [61] Zongfu Yu and Shanhui Fan, “Optical isolation based on nonreciprocal phase shift induced by interband photonic transitions,” *Applied Physics Letters* **94**, 171116 (2009).
- [62] Jingjing Yu, Huajin Chen, Yongbin Wu, and Shiyang Liu, “Magnetically manipulable perfect unidirectional absorber based on nonreciprocal magnetic surface plasmon,” *EPL (Europhysics Letters)* **100**, 47007 (2012).
- [63] Alexander B. Khanikaev, S. Hossein Mousavi, Gennady Shvets, and Yuri S. Kivshar, “One-way extraordinary optical transmission and nonreciprocal spoof plasmons,” *Phys. Rev. Lett.* **105**, 126804 (2010).